Sensor-free Corner Shape Detection by Wireless Networks

Yuxi Wang[†], Zimu Zhou[†], and Kaishun Wu[†‡]

[†]CSE Department, Guangzhou HKUST Fok Ying Tung Research Institute, HKUST

[‡]College of Computer Science and Software Engineering, Shenzhen University

{ywangav, zzhouad, kwinson}@cse.ust.hk

Abstract—**Due to the rapid growth of the smartphone applications and the fast development of the Wireless Local Area Networks (WLANs), numerous indoor location-based techniques have been proposed during the past several decades. Floorplan, which defines the structure and functionality of a specific indoor environment, becomes a hot topic nowadays. Conventional floorplan techniques leverage smartphone sensors combined with WiFi signals to construct the floorplan of a building. However, existing approaches with sensors cannot detect the shape of a corner, and the sensors cost huge amount of energy during the whole floorplan constructing process. In this paper, we propose a sensor-free approach to detect the shape of a certain corner leveraging WiFi signals without using sensors on smartphones. Instead of utilizing traditional wireless communication indicator Received Signal Strength (RSS), we leverage a finer-grained indicator Channel State Information (CSI) to detect the shape of a certain corner. The evaluation of our approach shows that CSI is more robust in sensor-free corner shape detection, and we have achieved over 85% detection accuracy in simulation and over 70% detection accuracy in real indoor experiments.**

Keywords—*Wireless, Channel State Information, Smartphone, Localization, Floorplan*

I. INTRODUCTION

Location based services (LBS) in indoor environment (e.g. floorplan, localization) have received increasing attention with the rapid development of wireless technology. New types of indoor mobile applications are being developed, covering a wide range of indoor personal and social scenarios. A key requirement to these location-based applications is the availability of a map which displays the user location.

In the case of indoor location-based applications, we need a floorplan. Whereas in outdoor applications, a street map is needed. Traditionally, outdoor location-based service providers (e.g. Google Maps, Baidu Maps) provide outdoor street maps for almost all regions [1]. However, the indoor equivalent floorplans are currently extremely limited, which places restrictions on the ubiquity and spread of indoor location-based applications. Recently, researches have been conducted to build indoor floorplan in efficient approaches. However, acquiring indoor floorplan information is challenging, since many buildings do not have floorplans in easily-interpretable digital form, and the internal structures together with the corresponding functionalities inside a building often evolve over time. Therefore, only few researches have made progress in indoor floorplans so far.

Conventional methods construct the floorplan by leveraging sensors (e.g. accelerator, gyroscope) on smartphones

and WiFi data. However, current methods can only recover corners whose shape is right-angled due to the inaccuracy of smartphone sensors, and they cannot detect the exact shape of a corner sometimes, which is a serious limitation [2]. Moreover, to detect the shape of a corner, sensors on smartphones must be kept on all the time during the entire detection period, which costs plenty of energy in smartphone location-based services [3]. Fig. 1 presents the ichnography layout of the Yellow River Hall and its adjacent rooms on the third floor of the Shanghai International Convention Center. Conventional floorplan methods, which leverage smartphone sensors and WiFi signals, can only construct the layout of the corridor shape the same as that shown in dash lines. However, compared with the actual floor layout, some of the constructed corridor positions are inside the rooms where people cannot reach in real life scenarios. To deal with the limitation in corner shape detection of the conventional floorplan methods and to manage energy efficiency on smartphones, we propose a sensor-free corner shape detection approach by leveraging WiFi signals with physical layer information only.
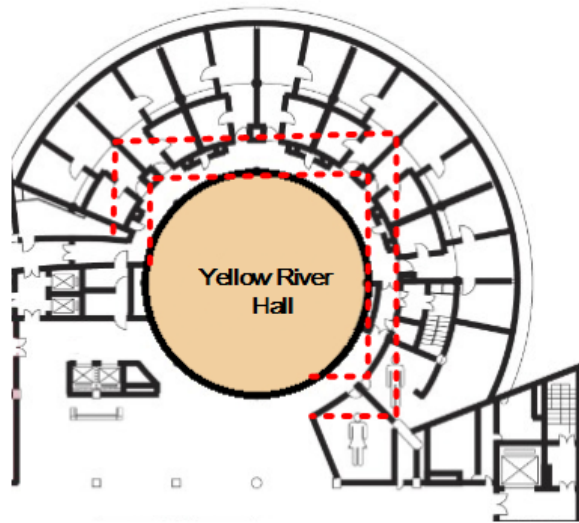

Fig. 1: Example of a Corner Shape Wrong Detection

Different from conventional floorplan approaches, we leverage wireless signals as indicator to perform corner shape detection. However, to detect the real corner shape using wireless signals is challenging since there are various wireless signals and they are sensitive to indoor environment. In our approach, we leverage physical layer Channel State Information

(CSI) instead if Received Signal Strength used in conventional indoor LBS services, and decide the shape of the corner by comparing the CSI variation pattern with that of each defined corner shape. To the best of our knowledge, this is the first work to detect corner shape using WiFi data only. We perform both simulation and real indoor experiments on RSS and CSI to classify the corner shapes into the following three types: straight-line, right-angle, and quadrant-arc. The simulation and experimental results show that our sensor-free corner shape detection approach leveraging CSI is accurate and efficient.

The rest of the paper is organized as follows. In Section II, we provide the preliminary work including channel models for simulation, together with an overview of Channel State Information. We present the detailed methodology of this work in Section III, which describes the detailed design of the work. After that, we provide the simulation and experimental results on both RSS and CSI of this work in Section IV, followed by the related work in Section V. Finally, in Section VI, we draw a conclusion on this paper.

II. PRELIMINARY

Channel modeling and measurement are fundamental for wireless communication. In this section, we provide a quick review on two typical channel models that will be used for our simulation, and Channel State Information (CSI), a fine-grained channel measurement on OFDM based WiFi devices for our scheme design and evaluation.

A. Channel Models

Ideally, the received signal power $P_r(d)$ at a propagation distance of d is calculated by Friis free space equation [4]:

$$P_r(d) = \frac{P_t G_t G_r \lambda^2}{(4\pi)^2 d^2} \qquad (1)$$

where P_t, G_t and G_r are the transmitted power, transmitter and receiver antenna gain, respectively. λ is the wavelength in meters. The Friis free space model only considers Line-Of-Sight (LOS) propagation. In typical indoor environments, however, signals transmit through multiple reflected or scattered paths (i.e. Non-Line-Of-Sight, NLOS paths). In this paper, we resort to two more generalized channel models for simulation.

1) Log-normal Shadowing: Log-normal shadowing model is adopted to predict average large-scale path loss for a wide range of environments as a function of propagation distance d and path loss exponent n:

$$PL(d) = PL(d_0) + 10n\log(d) + X_\sigma \qquad (2)$$

where $PL(d)$ is the power at distance d, $PL(d_0)$ is the power at close-in reference distance d_0, and X_σ is a zero-mean Gaussian distributed random variable with standard deviation σ. We apply log-normal shadowing model in our simulation for the case of slight multipath propagation.

2) Rayleigh Fading: When signal propagation is dominated by multipath, the channel exhibits Rayleigh fading. When the environment is rich in multipath, each path is modeled as a circularly symmetric complex Gaussian random variable by the Central Limit Theorem. The form of a circularly symmetric complex Gaussian random variable is:

$$Z = X + Yj,$$

where X and Y are zero mean i.i.d. Gaussian random variables. For a circularly symmetric complex Gaussian random variable Z,

$$E[Z] = E[e^{j\theta}Z] = e^{j\theta}E[Z],$$

The statistics of this variable can be specified by the variance,

$$\sigma^2 = E[Z^2],$$

The magnitude $|Z|$ is called a Rayleigh random variable, which has a probability density:

$$p(z) = \frac{z}{\sigma^2} e^{\frac{-z^2}{2\sigma^2}} \qquad (3)$$

Rayleigh fading model assumes that the signal magnitude fades according to Rayleigh distribution. And we apply Rayleigh fading model to simulate our corner shape detection scheme under rich multipath conditions.

B. Channel State Information

MAC layer Received Signal Strength (RSS) is widely adopted as an indicator for channel quality. As the superposition of multiple paths, RSS tends to be a fickle and unreliable channel measurement for both wireless communication [5] and indoor localization [6].

Modern modulation such as Orthogonal Frequency Division Multiplexing (OFDM) has revealed channel measurements at the granularity of subcarrier in the form of Channel State Information (CSI). CSI depicts the amplitude and phase of each subcarrier, and characterizes frequency selective fading due to multipath propagation. In a narrowband flat-fading channel, the OFDM system in the frequency domain is modeled as:

$$y = Hx + n \qquad (4)$$

where y is the received vector, x is transmitted vector, H is the channel matrix, and n is the additive white Gaussian noise (AWGN) vector. The CSI matrix of all subcarriers, which is an estimation of the matrix H in the above formula, can be estimated as:

$$\hat{H} = \frac{y}{x}$$

Leveraging the off-the-shelf Intel 5300 network card with a publicly available driver [7], a group of CSIs of 30 subcarriers are exported to the upper layer, and the CSI of a single subcarrier can be mathematically represents as:

$$h = |h|e^{j\sin\theta} \qquad (5)$$

where $|h|$ and θ are the amplitude and phase of the CSI subcarrier, respectively.

Compared with RSS, CSI provides finer-grained channel measurements, and can resolve multipath via frequency diversity [6]. Thus we employ CSI to eliminate multipath interference in our corner shape detection scheme.

III. METHODOLOGY

RSS or CSI is a function of the distance from the transmitter to the receiver for a typical indoor environment. When the receiver passes the corner at a constant moving speed, different corner shapes will lead to different RSS or CSI changing rates. Generally, the corner shapes inside a building can be classified as the following types: straight-line, right-angle, and quadrant-arc, shown in Fig. 2. This section depicts the methodology to distinguish the above three corner shapes via wireless networks. We first provide the feasibility of distinguishing corner shapes using wireless networks. Then, we present the CSI propagation model in indoor environment, which is utilized to simulate the CSI changing rate for different corner shapes. Finally, we provide a brief introduction on Gaussian smoothing used to filter the noise of the simulated and collect RSS and CSI signals in our approach, and the max correlation method to classify a specific corner shape as one of the defined three corner shapes in Fig. 2.
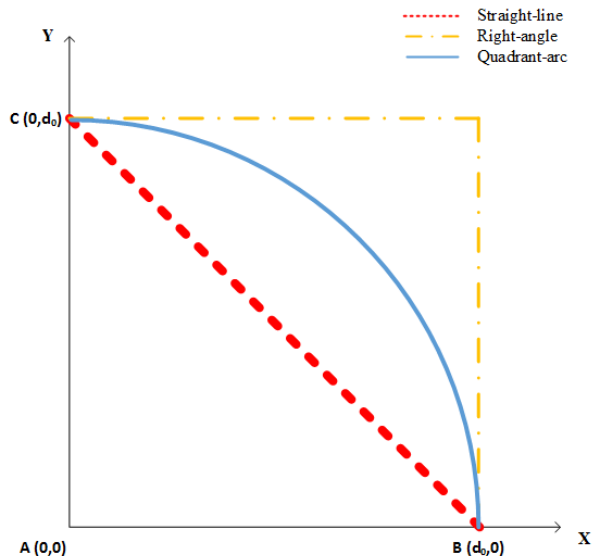

Fig. 2: Corner Shapes

A. Free Space Path Loss

In a typical indoor environment, there is one line-of-sight (LoS) path, which suffers the free space path loss. Meanwhile, due to the reflection of the surroundings such as floor, ceiling and walls, there exist several non-line-of-sight (NLoS) paths. This multipath propagation phenomenon causes constructive and destructive interference, and phase shifting of the signal.

Under idealized conditions, considered the path loss of LoS path only, the received power at the receiver antenna is given by the Friis free space equation [4]:

$$P_r(d) = \frac{P_t G_t G_r \lambda^2}{(4\pi)^2 d^2},$$

where $P_r(d)$ is the received power, d is the distance from the transmitter to the receiver, P_t is the transmitted power, G_t is the transmitter antenna gain, G_r is the receiver antenna gain, λ is the wavelength in meters and d is the distance from transmitter to receiver in meters.

When the receiver is passing the corner at a constant moving speed, the shape of the corner will lead to different power changing rates among the paths. Fig. 3a shows the theoretical power changing rate of different corner shapes when transmitter is placed at $(0,0)$. It is obvious that there are relationships between the receiver antenna's received power changing rates Rs of different shapes with respect to the time t, which can be formulated as:

$$R_{SL} = \frac{P_r G_t G_r \lambda^2}{(4\pi)^2(v^2t^3 - \sqrt{2}d_0vt^2 + d_0^2t)} \tag{6}$$

$$R_{RA} = \begin{cases} \frac{P_r G_t G_r \lambda^2}{(4\pi)^2(v^2t^3 + d_0^2t)}, & t \in (0, \frac{d_0}{v}), \\ \frac{P_r G_t G_r \lambda^2}{(4\pi)^2(v^2t^3 - 4d_0vt^2 + 5d_0^2t)} & t \in (\frac{d_0}{v}, \frac{2d_0}{v}) \end{cases} \tag{7}$$

$$R_{QA} = \frac{P_r G_t G_r \lambda^2}{(4\pi)^2(d_0^2t)} \tag{8}$$

where d_0 is the distance from the transmitter to the start point of the receiver, v is the specific speed which is constant, and R_{SL}, R_{RA}, and R_{QA} represent the power changing rates of shape Straight-line, Right-angle, and Quadrant-arc, respectively. The power changing rates of different shapes can form into different power changing rate patterns. Therefore, the corner shapes can be distinguished by leveraging the patterns of power changing rate.

Apart from the corner shape, the location of the transmitter AP also affects the received power changing pattern. Assume the receiver passes the corner from point A to point B in Fig. 2 along the three defined paths, and we define A as the 'starting-point' and B as the 'ending-point'. The power changing patterns of the three corner shapes become similar when AP is closed to either starting-point or ending-point. As shown in Fig. 3, if we define the distance between $(0,0)$ and the starting-point/ending-point as 5m, when AP is placed at $(0,0)$ or $(0,2)$, we can still distinguish the corner shapes using power changing patterns theoretically. However, the power changing patterns of different shapes become similar when AP is placed at $(0,4)$. By observation, Fig. 4 shows that when setting the location of AP on x-axis/y-axis with the distance to origin point d_{AP} no more than $0.4d_0$, we can distinguish the corner shapes leveraging power changing patterns even with little noise, where d_0 is the distance between origin point $(0,0)$ and the starting-point/ending-point in Fig. 2. However, power changing pattern cannot help in shape detection when d_{AP} becomes larger. Therefore, in this paper, we define an effective zone for the location of AP in our approach, which requires d_{AP} is no more than $0.4d_0$. In the rest of this paper, we only consider scenarios under the effective zone condition.

B. Distinguish Corner Shape with CSI

The radio propagation model for RSS is not suitable for CSI since it is obtained from the baseband on the receiver, the models described above cannot be used for the relationship between the path shape and the CSI value at unit time. In [6], the authors proposed a refined indoor propagation model to represent the relationship between CSI and the distance d. Given a packet with 30 groups of subcarriers, the effective CSI
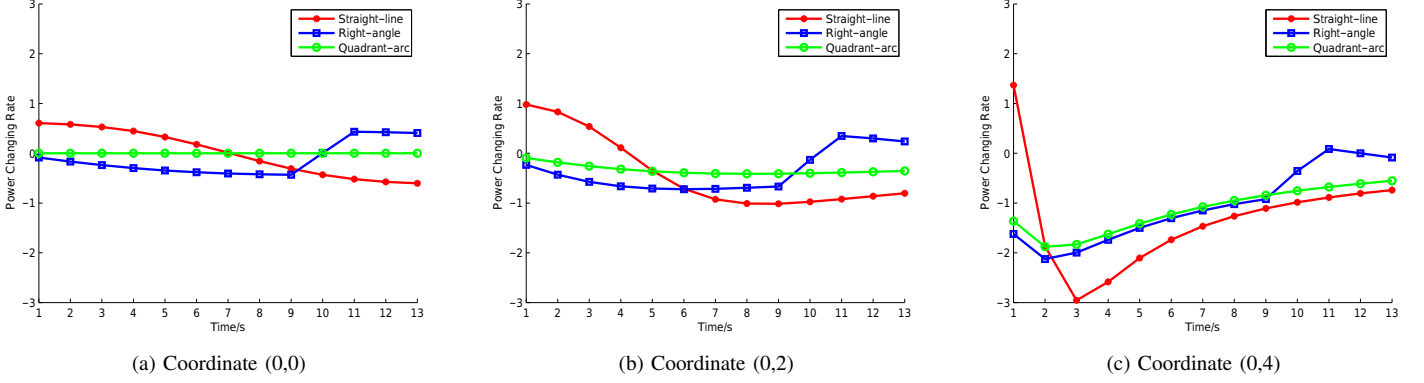
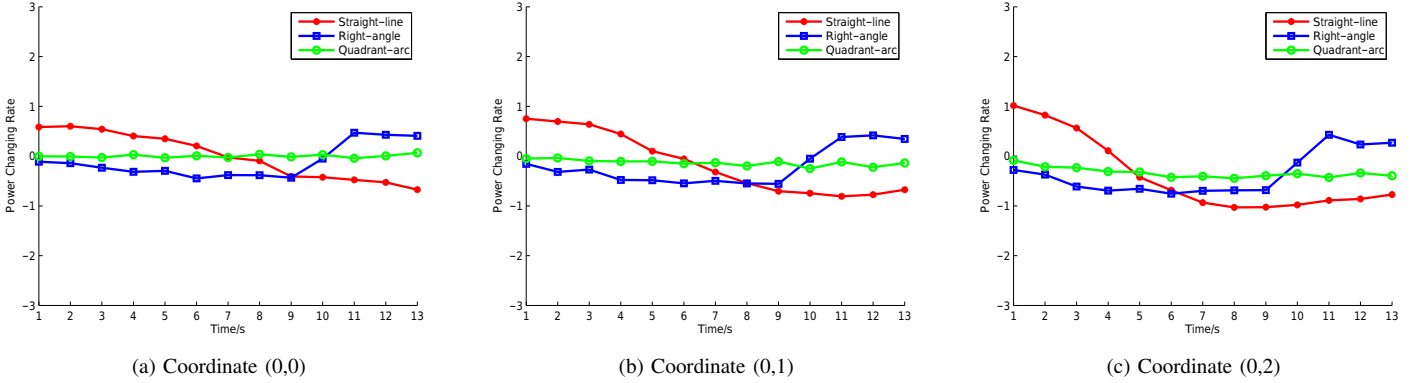Fig. 3: Theoretical Power Changing Rate Patterns at coordinate (0,0), (0,2), and (0,4)

Fig. 4: Power Changing Rate Patterns with noise at coordinate (0,0), (0,1), and (0,2)

of this packet is given as:

$$CSI_{eff} = \frac{1}{K}\sum_{k=1}^{K}\frac{f_k}{f_0} \times |A|_k, k \in (-15, 15), \qquad (9)$$

where K is the number of subcarriers, f_0 is the central frequency, f_k is the frequency of the k-th subcarrier, and $|A|_k$ is the amplitude of the k-th subcarrier. The distance from the transmitter to the receiver is calculated as:

$$d = \frac{1}{4\pi}\left[\left(\frac{c}{f_0 \times |CSI_{eff}|}\right)^2 \times \sigma\right]^{\frac{1}{n}}, \qquad (10)$$

where c is the wave velocity, σ is the environmental factor and n is the path loss fading exponent. We leverage this proposed model to establish the relationship between path shape and CSI.

C. Decision of Corner Shape

To distinguish the corner shapes leveraging the received power changing pattern, we choose to use max correlation method. In our approach, we store the power changing patterns of each corner shape at various AP locations within the effective zone in a training data matrix. Each row of the matrix represents the power changing pattern of a certain corner shape

for a specific AP location. When a new set of test data comes in, we compute the correlation value between the test data and the data of each row in the training matrix. The corner shape type with the highest correlation value is chosen as the type for the testing corner shape data. To make the detection more precise, we leverage Gaussian smoothing to filter the noise of the signals before detection. Gaussian filter modifies the input signal by convolution with a Gaussian function to remove the noise.

We simulate the Wi-Fi propagation leveraging Log-normal Shadowing model and Rayleigh Fading model for RSS, and using CSI propagation model in [6] for CSI simulation. We also conduct experiments to evaluate the relationship between path shape and RSS or CSI in real indoor environment.

IV. EXPERIMENTS AND RESULTS

In this section, we presents the results of RSS and CSI simulations with different propogation models, and the results of RSS and CSI experiments in real indoor environment.

A. Experiment Setup

The simulation platform is Matlab 2013a installed on a 3.40GHz Intel(R) Core(TM) i7-4770 CPU 16G RAM desktop.

Log-normal Shadowing model is selected to simulate the signal propagation for an indoor environment with less multipath effect, and Rayleigh Fading model for an rich multipath indoor environment.

The experiments are conducted in a lobby area in the campus of the Hong Kong University of Science and Technology. We leverage a TP-LINK TL-WDR4300 wireless router with 3 detectable antennas as the transmitter, and a 3.20GHz Intel(R) Pentium 4 CPU 2GB RAM desktop equipped with Intel 5300 NIC as the receiver. The transmitter operates in IEEE 802.11n AP mode at 5GHz. The receiver has 3 working antennas and the firmware is modified as in [5] to report CSI to upper layer. RSS is calculated using CSI. During the experiment, the receiver continuously pings packets from the AP at the rate of 100 packets per second.

In both simulation and experiments, we define d_0 in Fig. 2, which is the distance between the origin point (0,0) and the starting-point/ending-point, as 5m. AP is set to be placed at (0,0), (0,1), (0,2), (1,0) and (2,0) during simulation, and is placed only at the origin point (0,0) during the entire experiment. The moving speed of the receiver is defined as 0.5m/s, and we set one reference point on the paths representing different corner shapes every second corresponding to the moving speed. Since different corner shapes lead to different time duration of passing the corner, we only select data within the shortest corner passing time duration (14s) for evaluation. The power changing rate for evaluation is defined as the slope of the received power waveform.

B. Simulation Results

In this section, we describe the simulation results of RSS under Log-normal Shadowing Model and Rayleigh Fading Model, as well as simulation results of CSI.

1) RSS Log-normal Shadowing Simulation: Log-normal Shadowing Model is chosen to simulation the corner shape detection using RSS in an indoor environment with slight multipath effect. We first filter the noise of the signal data, and then calculate the correlation between each type in training data matrix and the test data. TABLE I shows the correlation value between the training data matrix and five groups of test data of Straight-line shape which are selected randomly. From the table, we can obviously figure out that the correlation values in column "Straight-line" are around 0.9, which means the test data almost has a perfect direct linear relationship with the training data of type "Straight-line". Meanwhile, from the values in the other two columns, we know that there is weak perfect increasing linear relationship between the test data and the training data of other two types. Therefore, we classify the test data into type "Straight-line". For the other groups of test data, we can also use the max correlation method to classify them into specified types.

Fig. 5 shows the corner shape detection predict rates with respect to the corresponding types of the three defined corner shapes. The simulation shows that in an indoor environment with slight multipath effect, the predict rates of shape Straight-line and Right-angle are both 99%, and the predict rate of corner shape Quadrant-arc is 93.8% even using RSS as the transmission indicator. Therefore, it can be concluded that it is reliable to utilize RSS to distinguish the corner shape using

TABLE I: Correlation of Three Defined Types with Test Data of Straight-line using Log-normal Shadowing Model

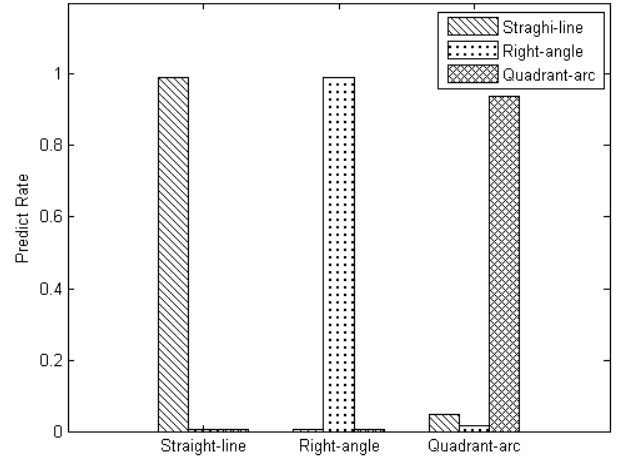| Type	STRAIGHT-LINE	RIGHT-ANGLE	QUADRANT-ARC
Data1	0.916	-0.524	0.555
Data2	0.913	-0.511	0.537
Data3	0.892	-0.533	0.496
Data4	0.942	-0.542	0.549
Data5	0.931	-0.542	0.549

Fig. 5: Predict Rates of Different Corner Shapes for Log-normal Model

the max correlation method from the defined three types in an ideal environment.

2) RSS Rayleigh Fading Simulation: Rayleigh Fading Model is chosen to simulation the corner shape detection using RSS in an indoor environment with rich multipath effect. We calculate the correlation values after filter the noise of the signals using Gaussian smoothing. Fig. 6 shows the corner shape detection predict rates of the three defined corner shapes.

The simulation shows the predict rate using RSS as indicator in an indoor environment with rich multipath effect, which is the common indoor scenarios in real life. The figure shows that the predict rate of shape Straight-line is 46%, and the rate of Right-angle is 47%. Although the predict rate of Quadrant-arc is a little bit higher, which is about 61%. Therefore, we can conclude that it is unreliable to utilize RSS to distinguish the corner shape from the defined three types in real cases.

3) CSI Simulation Result: Since we have proved that RSS is unreliable to be used as the indicator in corner shape detection in real cases, a finer-grained indicator CSI is a reasonable choice for us. We simulate the CSI-based corner shape detection by leveraging the model proposed in [6], which is a well-defined model for CSI propagation in rich multipath effect indoor environment.
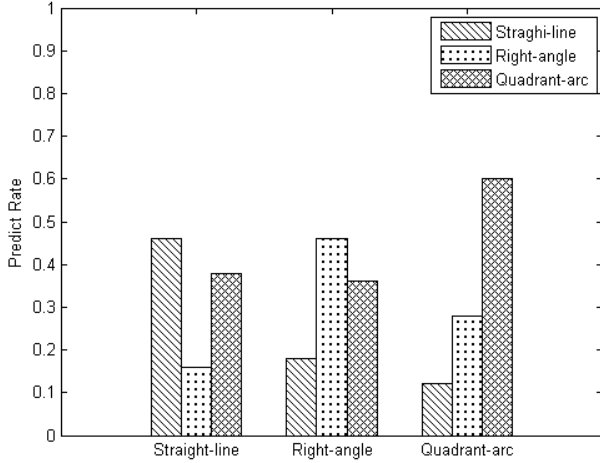
Fig. 6: Predict Rates of Different Corner Shapes for Rayleigh Model

Fig. 8: Power Changing Rate of Experimental RSS Data

Fig. 7 shows the predcit accuracies using CSI as the indicator in a real indoor environment with rich multipath effect with the model proposed in [6]. The figure shows that the predict rate of shape Straight-line is 92%, the rate of Right-angle is 90%, and the predict rate of Quadrant-arc is 87%. Though the predict accuracies are not as high as those with Log-normal Shadowing model and RSS, the accuracies are all above 85%, which is acceptable. Therefore, the simulation results can illustrate that corner shape detection using CSI is reliable in indoor environment with rich multipath.
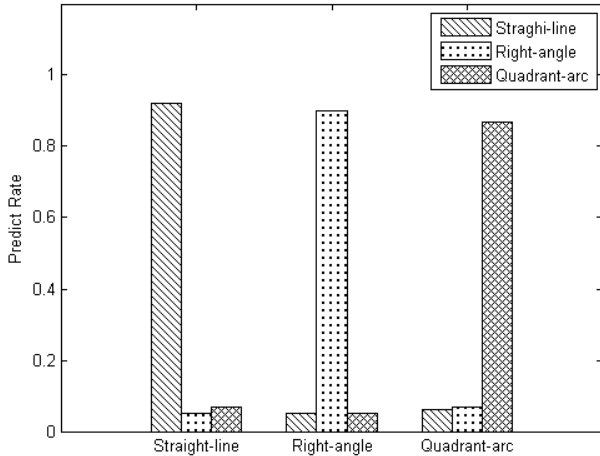
Fig. 8 shows the power changing rate of a group of RSS values calculated from CSIs, which is selected randomly. Since multipath effect has strong influence on RSS, it cannot keep its theoretical power changing pattern. Therefore, we cannot leverage RSS to detect the corner shape in real experiment. Fig. 9 shows the power changing rates of RSS and CSI of Quadrant-arc shape compared with power changing rate simulated using Log-normal Shadowing model. It is obviously that CSI has a more similar power changing pattern than RSS. Fig. 10 shows the predict rates using CSI. We can achieve over 70% of the predict accuracy, which is acceptable.

Fig. 7: Predict Rates of Different Corner Shapes using CSI

Fig. 9: Shadowing Model, CSI and RSS Power Changing Rate Comparison of Quadrant-arc

C. Experimental Results

We conduct experiments in an open lobby environment, and collect CSIs for evaluation. We first use Gaussian Filter to filter the noise of the collected data. The filtered CSIs are used for experimental evaluation. The RSS values used for evaluation are calculated from the filtered CSIs.
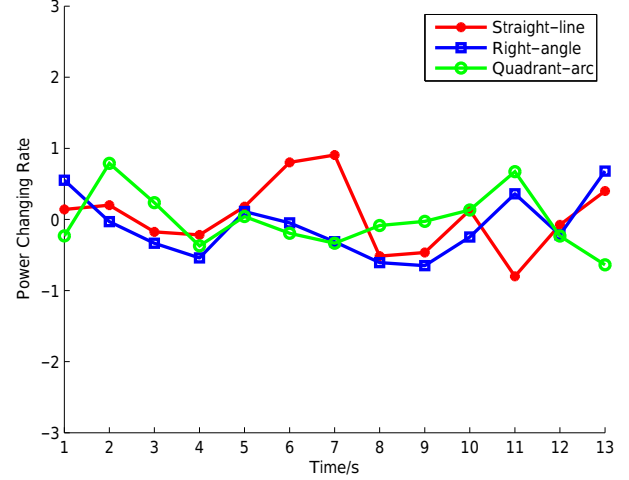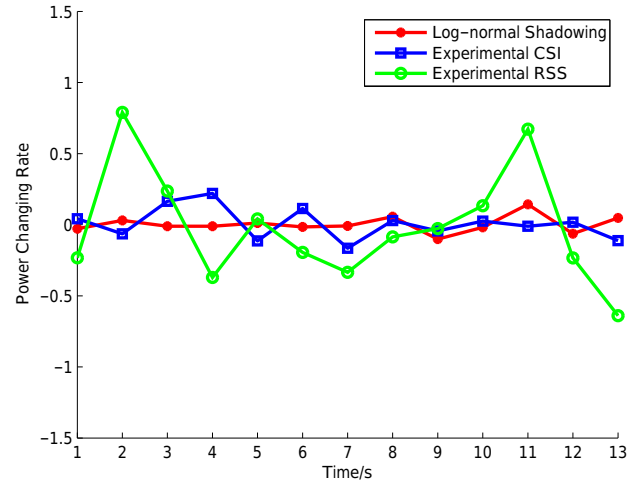
V.   RELATED WORK

This work is closely related to the following two research categories.

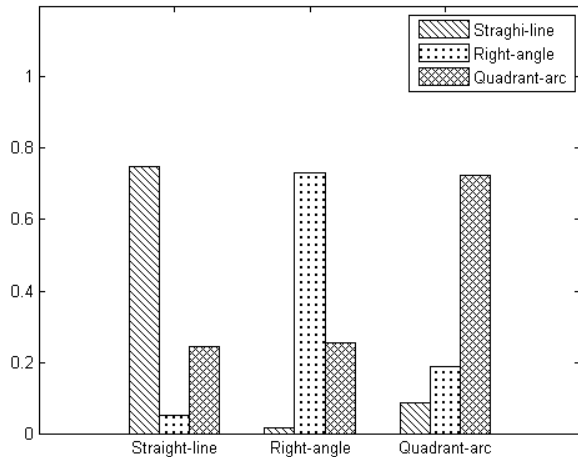**Floor Plan Construction.** Floor plan is a key pre-requisite

Fig. 10: Experimental CSI Predict Rates of Different Shapes

for various indoor location based services, yet is not always available. Extensive research in robotics has explored Simultaneous Localization and Mapping (SLAM) techniques [8], while a new trend is to automatically construct the floor plan with sensor-rich smartphones in a crowdsourced manner [9] [2] [10] [11]. The main principle is to combine and segment multiple user trajectories into hallways and rooms by unique physical (e.g. elevator and stairs) [9] or wireless landmarks [10] [11]. However, due to the noisy data of phone-embedded inertial sensors and the unconstrained orientation of smartphones [12], inertial based trajectories are often segmented by right-angled turns, and most floorplan construction schemes degrade in case of curved hallways or irregular shapes [11]. Our work is inspired by this thread of research and serves as a complement for inertial based turn/corner detection schemes. We exploit the unique received signal characteristics of WiFi to infer curved or right-angled hallway structures, as radio propagation trend is more stable w.r.t. human locomotion.

CSI-based Indoor Localization. Multipath effect resides as a primary challenge for wireless indoor localization. An emerging trend to combat such phenomenon is to leverage finer-grained Channel State Information (CSI), which implicitly characterizes multipath propagation via frequency diversity [13]. CSI helps to extract the power of the dominant (often line-of-sight) path for accurate ranging [6], angle-of-arrival estimation [14], and has also been employed to infer line-of-sight propagation [15] and calculate path loss exponent [16]. In this work, we also utilize CSI to extract the power of the direct propagation path. But instead of using the signal power at a fixed location to estimate propagation distance or direction, we exploit the signal power trend of the direct path along a trajectory to infer the geometric structure of the hallway.

VI. CONCLUSION

Understanding the indoor environments is important for a wide range of mobile personal and social applications, which often requires knowledge of indoor floorplans. Conventional floorplan approaches leverage smartphone sensors combined with wireless signals to construct the indoor map of a building, which causes a serious limitation that they cannot detect the real shape of a corner shape precisely. In this paper, we propose a trivial sensor-free method to detect the corner shape. Our approach leverages physical-layer information CSI to classify the shapes of the corners into the defined three types. This approach can also save the energy consumption caused by smartphone sensors, and has achieved promising corner shape detection accuracy.

REFERENCES

[1] H. Li and L. Zhijian, "The study and implementation of mobile gps navigation system based on google maps," in *Computer and Information Application (ICCIA), 2010 International Conference on*. IEEE, 2010, pp. 87–90.

[2] H. Shin, Y. Chon, and H. Cha, "Unsupervised Construction of an Indoor Floor Plan using a Smartphone," *IEEE Transactions on Systems, Man, and Cybernetics, Part C: Applications and Reviews*, vol. 42, no. 6, pp. 889–898, 2012.

[3] Z. Zhuang, K.-H. Kim, and J. P. Singh, "Improving energy efficiency of location sensing on smartphones," in *Proceedings of the 8th international conference on Mobile systems, applications, and services*. ACM, 2010, pp. 315–330.

[4] T. S. Rappaport *et al.*, *Wireless Communications: Principles and Practice*. Prentice Hall PTR New Jersey, 1996, vol. 2.

[5] D. Halperin, W. Hu, A. Sheth, and D. Wetherall, "Predictable 802.11 Packet Delivery from Wireless Channel Measurements," in *Proce. of ACM SIGCOMM*, 2010.

[6] K. Wu, J. Xiao, Y. Yi, M. Gao, and L. M. Ni, "FILA: Fine-grained Indoor Localization," in *Proc. of IEEE INFOCOM*, 2012.

[7] D. Halperin, W. Hu, A. Sheth, and D. Wetherall, "Tool Release: Gathering 802.11n Traces with Channel State Information," *ACM SIGCOMM Computer Communication Review*, vol. 41, no. 1, p. 53, 2011.

[8] H. Durrant-Whyte and T. Bailey, "Simultaneous Localization and Mapping: Part I," *IEEE Robotics Automation Magazine*, vol. 13, no. 2, 2006.

[9] M. Alzantot and M. Youssef, "Crowdinside: Automatic Construction of Indoor Floorplans," in *Proc. of ACM GIS*, 2012.

[10] G. Shen, Z. Chen, P. Zhang, T. Moscibroda, and Y. Zhang, "Walkie-Markie: Indoor Pathway Mapping Made Easy," in *Proc. of USENIX NSDI*, 2013.

[11] Y. Jiang, Y. Xiang, X. Pan, K. Li, Q. Lv, R. P. Dick, L. Shang, and M. Hannigan, "Hallway based Automatic Indoor Floorplan Construction using Room Fingerprints," in *Proc. of ACM UbiComp*, 2013.

[12] R. Harle, "A Survey of Indoor Inertial Positioning Systems for Pedestrians," *IEEE Communications Surveys Tutorials*, vol. 15, no. 3, pp. 1281–1293, 2013.

[13] Z. Yang, Z. Zhou, and Y. Liu, "From RSSI to CSI: Indoor Localization via Channel Response," *ACM Computing Surveys*, vol. 46, no. 2, pp. 25:1–25:32, 2013.

[14] S. Sen, R. R. Choudhury, and S. Nelakuditi, "SpinLoc: Spin Once to Know Your Location," in *Proc. of ACM HotMobile*, 2012.

[15] Z. Zhou, Z. Yang, C. Wu, W. Sun, and Y. Liu, "LiFi: Line-Of-Sight Identification with WiFi," in *Proc. of IEEE INFOCOM*, 2014.

[16] S. Sen, J. Lee, K.-H. Kim, and P. Congdon, "Back to the Basics: Avoiding Multipath to Revive Inbuilding WiFi Localization," in *Proc. of ACM MobiSys*, 2013.